Plastic Deformation at Surface During Unlubricated Sliding

Takashi Yamamoto and
Donald H. Buckley

NASA

Plastic Deformation at Surface During Unlubricated Sliding

Takashi Yamamoto and
Donald H. Buckley
*Lewis Research Center
Cleveland, Ohio*

Summary

The plastic deformation and wear brought about in the sliding process were observed by using a scanning electron microscope (SEM) and an optical microscope. An aluminum oxide rider was made to slide on a 304 stainless-steel disk surface. The disk surface was sputter-cleaned by argon discharge. Sliding experiments were conducted in a vacuum of 10^{-6} Pa and in an environment of 5×10^{-4} Pa chlorine gas at 25° C. The load was 500 grams and the sliding velocity was 0.5 centimeter per second.

Characteristic modes of deformation and fracture behavior were observed on the 304 stainless-steel disk surfaces. The deformed surface layer which accumulates and develops successively is left behind the rider, and step-shaped protuberances are developed even after single-pass sliding under both environmental conditions. A fully developed surface layer is gradually torn off, leaving a characteristic morphological contour. These observations result from both adhesion and an adhesive wear mechanism, and their process of formation is explained from a morphological viewpoint.

Introduction

When two solid surfaces are brought into contact and relative motion occurs between those surfaces due to sliding, rolling, or rubbing, friction and wear can result. Friction behavior of solid materials is more fully understood on the basis of several principal concepts of tribological surface properties, thin surface films, and real contact area. These concepts frame the so-called adhesion theory of friction. Careful observations of the wear process lead to the conclusion that material transfer occurs during unlubricated sliding contact for metals, and, that in certain cases, it is in fact even observed under the condition of lubricated sliding contact. Buckley (ref. 1) and Bowden and Tabor (ref. 2) have published fundamental information concerning the characteristics of an interfacial layer between two surfaces, which explains the material transfer occurring between contacting surfaces (refs. 1 and 2).

Although considerable information is presently available concerning adhesion of surfaces, the understanding of the wear mechanism is still somewhat unclear. This subject is still greatly debated, particularly with respect to how wear fragments are produced in the process of relative motion between contacting surfaces. The adhesive wear theory does not yet offer a suitable mechanism of wear fragment formation because proponents of the theory have a tendency to discuss it exclusively from an atomistic viewpoint. In most practical problems, contact occurs over a finite area far larger than the atomic scale. Therefore, a good deal of knowledge is needed for larger contact area as well as atomic size contact. It is necessary to establish the boundary conditions for the large-scale contact and to determine how the fundamental information obtained from the atomic scale can be applied. Such an investigation should assess the morphological behavior of the contact region. In this paper observations of plastic deformation occurring under ordinary sliding contact using scanning electron microscopy and optical microscopy are described from a morphological point of view.

# Experimental Apparatus and Procedure

Apparatus

The experiments were conducted in a vacuum chamber (fig. 1). The vacuum system was pumped by sorption pumps and an ion pump. Pressure in the vacuum system was read with an ion gage. The specimens consisted of a disk 6.5 centimeters in diameter and 1.2 centimeters thick and a roller-shaped rider with a spherical surface 2.5 centimeters in radius. The specimens are shown in the apparatus schematic in figure 1. The disk specimen was mounted on a drive shaft that was rotated by means of a magnetic drive assembly. The drive assembly provides for rotation speeds to 15 millimeters per second. The roller can be rotated with the friction force between the roller and the disk. In this study the rotation of the roller was held up by a stopper. Therefore, pure sliding was conducted at the contact surface.

The friction force working between the disk and the rider was continuously recorded during the experiment. The beam containing the rider specimen was welded in a bellows assembly that was gimbal-mounted to the vacuum system. The gimbal mounting permits deadweight loading of the rider against the disk surface. The beam containing the rider can move in two directions in the horizontal plane at right angles to the deadweight loading. As the disk rotated, movement of the rider was restricted by a cable attached to a temperature-compensated strain gage. These gages measured the friction force between the disk and the rider specimens.

Materials and Specimen Preparation

Two sets of specimens were used for this study. The disk material was 304 stainless steel (hardness about 260 Vickers hardness number), and the rider material is aluminum oxide. The environmental gas used in this study was 99.5 percent pure chlorine.

The rider specimens were acid-cleaned before use with aqua regia to remove metal and other contaminants that might have become embedded in the surface during finishing. They were then rinsed in water and finally rinsed in ethyl alcohol. The surface profile of the cleaned rider is shown in figure 2. Average peak-to-valley
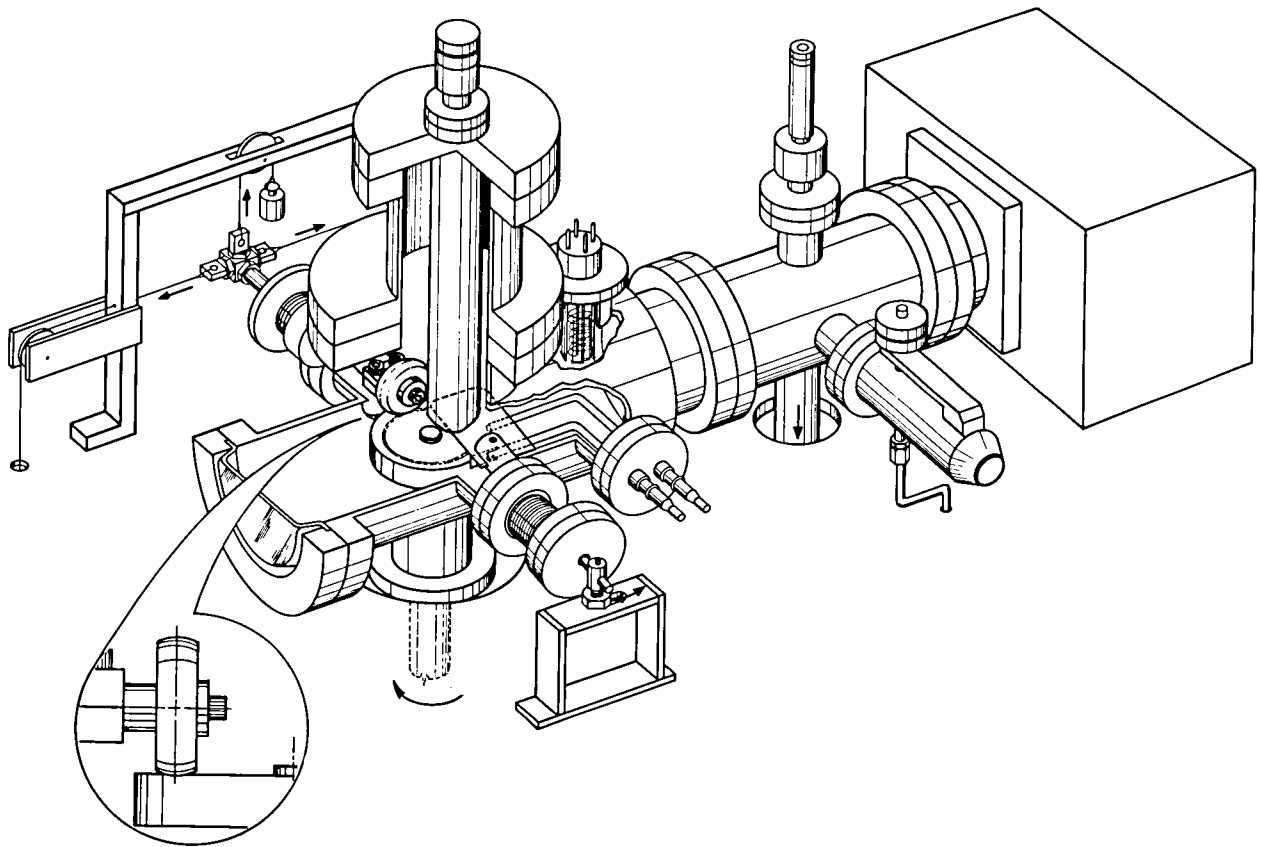
CD-81-12631

Figure 1. - Sliding and rolling contact apparatus with Auger spectrometer.
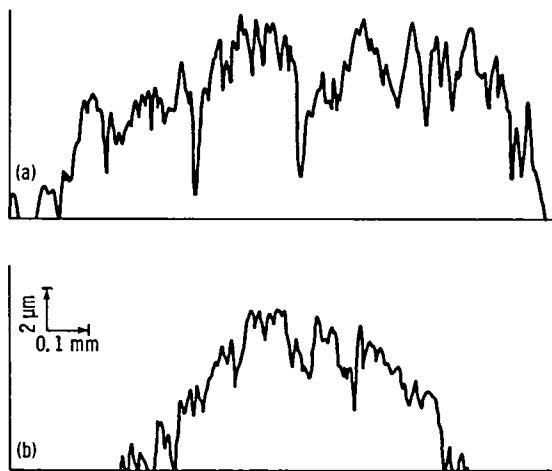
(a) Surface profile in axial direction.

(b) Surface profile in peripheral direction.

Figure 2. - Surface profiles of aluminum oxide rider.

roughness in the peripheral direction was about 2 micrometers.

The disk specimen surfaces were finish-ground on metallurgical papers to a grit of 600. They were diamond-polished with 6-micrometer and then with 3-micrometer diamond paste. The disk specimens were rinsed with Freon and then with absolute ethyl alcohol. The disk specimens were further cleaned by ion bombardment. In this process research-grade argon gas was bled into the system until a pressure of about 10 Pa was reached. A d.c. power supply was used to supply 750-volt differential between the disk and a floating electrode. The current under this condition was 60 milliamperes. With a negative potential on the disk, positively charged argon ions bombarded and sputter-cleaned the specimen surfaces. Sputtering was continued until only peaks for the elements in 304 stainless steel were detected by Auger spectroscopy. The rider surface was covered by a shield of 440C stainless steel to avoid contamination during ion bombardment as indicated in figure 1.

Procedure

Sliding experiments were conducted with the rider specimen loaded against the disk surface in a vacuum of 10^{-6} Pa and 5×10^{-4} Pa of chlorine gas. As the disk was rotated, the rider scribed a circular sliding track on the flat surface of the disk. The load used in this study was 500 grams, and the rotating speed of the disk specimen was 5 millimeters per second. The environmental temperature was 25° C.

Elemental analysis of the disk specimen surface was

made before and after the sliding experiments by using an Auger cylindrical-mirror analyzer with an integral electron gun. The beam of the electron gun could be positioned directly into the desired position of the wear contact zone by a sample scanning positioner with a television monitor.

Scanning electron microscope and optical microscope observations were conducted on the disk surfaces after one pass and after 50 sliding passes of the rider. One-pass and 50-pass sliding were carried out on the same disk specimen surface. The diameters of the sliding tracks were slightly different to avoid overlap. The depth of the groove and height of the plateau formed by sliding experiments were determined by adjusting the focus of a lens system of the high-magnification optical microscope.

Results

Before conducting sliding experiments, the 304 stainless-steel disk surfaces were examined with the Auger spectrometer with the normal oxides and adsorbates on the surface. A typical Auger spectrum is presented in figure 3(a). The elements sulfur, carbon, chlorine, oxygen, and iron were detected. The carbon can originate from two sources: from carbon monoxide and/or carbon dioxide adsorbed onto the surface; and from the stainless steel, in which it is an alloying element. The oxygen can result from adsorbates and iron or chromium oxide. Argon ion sputter-cleaning of the disk surface resulted in the Auger spectra of figures 3(b) and 4(a). Examination of the Auger spectra reveals only peaks for elements of the 304 stainless steel (i.e., Fe, Ni, Cr, C). The surface is free of oxygen, chlorine, and sulfur. Based on these patterns, the disk surface is atomically clean. In figure 4(b) an Auger spectrum is presented for a clean, stainless-steel surface after being saturated with chlorine by exposure to over 10^5 Langmuirs of chlorine gas. There are, in addition to the peaks of the stainless-steel elements, Auger peaks for chlorine.

Sliding experiments were conducted under two conditions: at 10^{-6} Pa with a clean disk, and at 5×10^{-6}
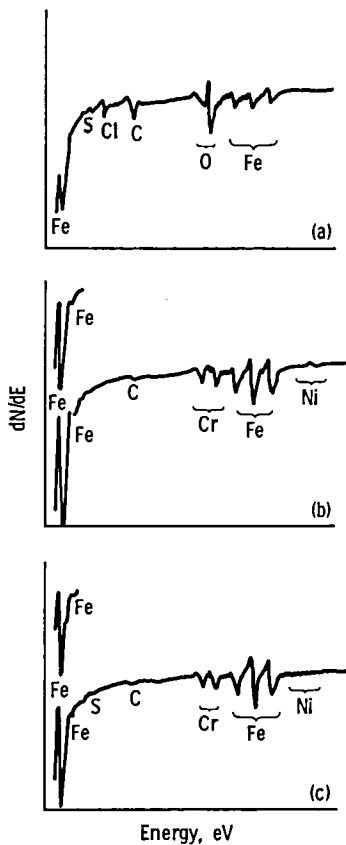
(a) Before sputter cleaning.

(b) After sputter cleaning.

(c) After 50 passes of aluminum oxide rider in 10^{-6}-Pa vacuum.

Figure 3. – Auger spectra for 304 stainless steel disk surface (I).
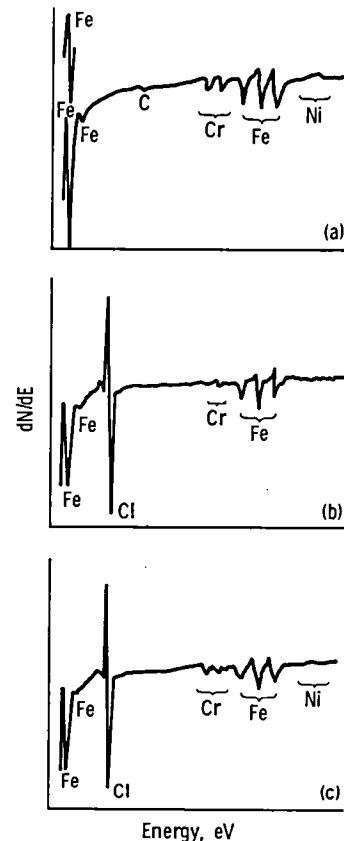
(a) Before sputter cleaning.

(b) After sputter cleaning.

(c) After 50 passes of aluminum oxide rider in 5×10^{-4}-Pa chlorine gas.

Figure 4. – Auger spectra for 304 stainless steel disk surface (II).

torr of chlorine gas with the disk surface saturated with chlorine. Examination of figures 3(b) and (c) and 4(b) and (c) indicates essentially no change in Auger peaks after 50 pass, although in the 10^{-6} Pa condition, an auger peak for sulfur was slightly detected after 50 passes (fig. 3(c)). One possible reason is contamination of the rider surface in the process of sputtering. The contaminant seems to transfer to the disk surface during 50 passes of sliding. However, this small amount of contamination has no observable effect on the surface deformation behavior.

Figures 5 and 6 show representative surfaces of the specimens tested at 10^{-6} Pa and at 5×10^{-4} Pa of chlorine gas. Even in the chlorine-gas environment, severe shearing and tearing can be observed on the disk surface. Transfer of wear fragments can also be observed on the rider surface under both conditions. Differences observed on the surfaces will be mentioned later using SEM photographs. Figure 7 represents examples of surface profile formed on the disk surface under the various sliding conditions.

Figure 8 indicates the variation of the friction coefficient with the number of passes of the rider. The initial average value of the friction coefficient was 1.2, but the establishment of a sliding track decreased the friction coefficient to a value 0.5 in the 10^{-6}-Pa environment. Fluctuation of the friction coefficient also gradually decreased with the number of passes. The friction coefficient, μ, changed from 1.0 to 0.4 at 5×10^{-4} Pa of chlorine gas. Again, the fluctuation decreased with the number of passes, but its width was narrower than that observed in a vacuum of 10^{-6} Pa. This behavior can be explained by the formation of surface films in the chlorine-gas environment.

Figures 5 to 7 show that the surface layer does not deform uniformly over the apparent contact width in the axial direction; this is especially clear in the one pass sliding results. The width of the sliding track formed in a vacuum of 10^{-6} Pa after 50 sliding passes is less than that formed in 5×10^{-4} Pa of chlorine gas. These variations are probably related to several factors involved in the experiment. The characteristic profile of the aluminum oxide rider (fig. 2), as formed in the machining process, is a possible factor. In this study attention was paid to the qualitative phenomena fundamental to wear mechanisms. It is not influenced by the nonuniformity in wear observed.

Scanning electron microscope (SEM) photographs of the deformed surface observed at the initiation of one pass sliding in a vacuum of 10^{-6} Pa are shown in figure 9. Figure 10 represents a typical portion of the sliding wear track after sliding some distance on the surface. The height and depth of the surface profiles are indicated in the photographs on the right as measures of the distance from the initial level of the disk surface. Two types of
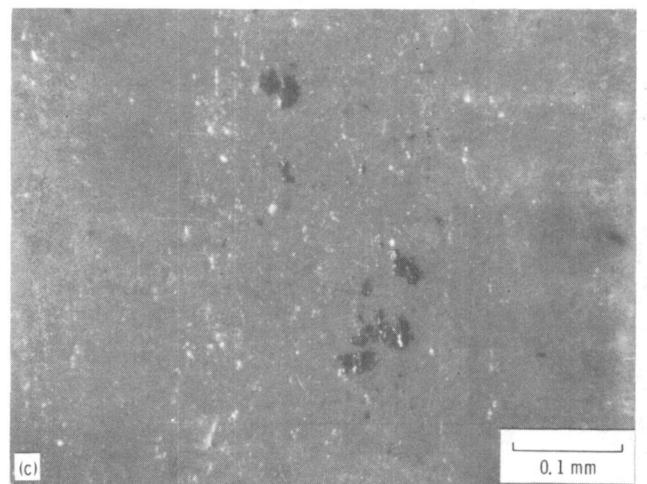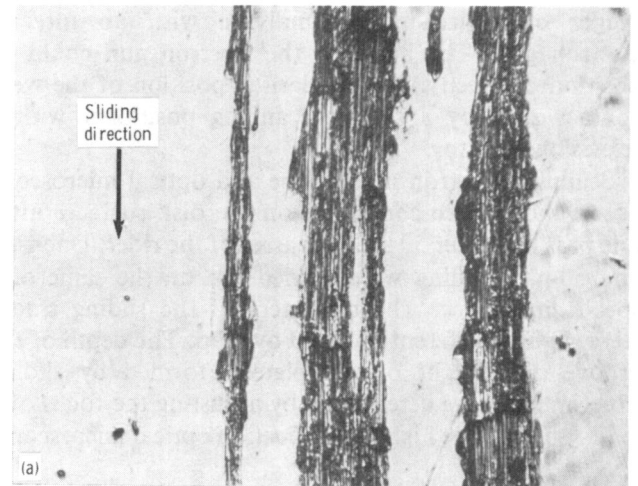

(a) Sliding track after one pass.

(b) Sliding track after 50 passes.

(c) Wear fragments transferred to rider surface after 50 passes.

Figure 5. - Optical micrographs of rider and disk surfaces after sliding in 10^{-6}-Pa vacuum.

(a) Sliding track after one pass.

(b) Sliding track after 50 passes.

(c) Wear fragments transferred to rider surface after 50 passes.

Figure 6. - Optical micrographs of rider and disk surfaces after sliding in 5x10⁻⁴-Pa chlorine gas environment.
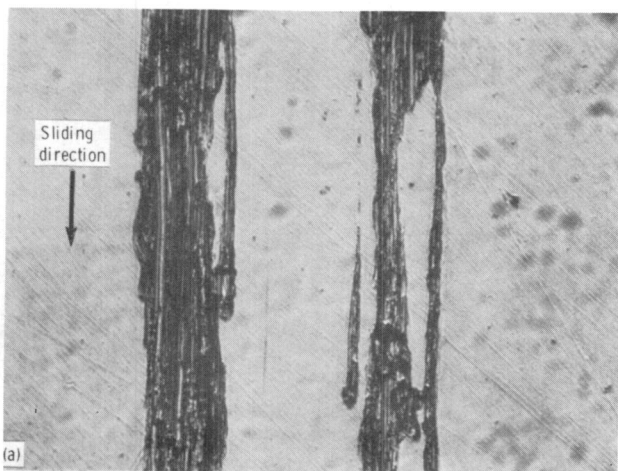
characteristic protuberances are observed on the sliding track shown in figure 10: one is isolated as an island, and the other is intermittently scattered on the track. The island-shaped protuberances are shown in the micrographs of figure 11 under magnification. Other examples taken at several different locations are shown in figure 12.

Figure 13 shows SEM photographs of the deformation observed in a 5×10^{-4} Pa chlorine gas environment. The results observed are substantially similar to those observed in a vacuum of 10^{-6} Pa. On all the disk surfaces, characteristic trapezoid-shaped or step-shaped protuberances are formed during the initial stage of sliding contact. Slip marks are visible on most upper surfaces of the protuberances.

The surface contour of the sliding track observed after 50 passes of the rider is shown in figures 14 and 15. The former was obtained in a vacuum of 10^{-6} Pa and the latter in an environment of 5×10^{-4} Pa chlorine gas. Photographs of the observed sliding tracks obtained by SEM can be compared with those obtained from the optical microscope and are shown in figure 16. The nonsliding area and isolated protuberances are observed on the surface after 50 passes of the rider even in the environment of 5×10^{-4} Pa chlorine gas (fig. 16). The protuberances exist in the contacting regions of the sliding surface, not in the unslid portion of the wear track. Results obtained under both the conditions of 10^{-6} Pa vacuum and 5×10^{-4} Pa chlorine gas indicate that the surface layer is gradually torn off and the surface takes on a characteristic geometry.

Examples of wear fragments found on the disk surface are shown in the SEM photographs of figure 17. The left photograph shows examples of large wear fragments found on the surface. A cracked area or flake, which would likely be torn off by subsequent sliding, can be also observed at the edge of the surface plateau.
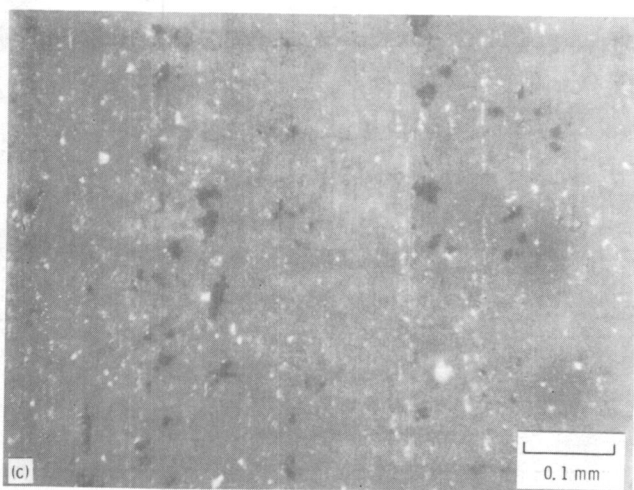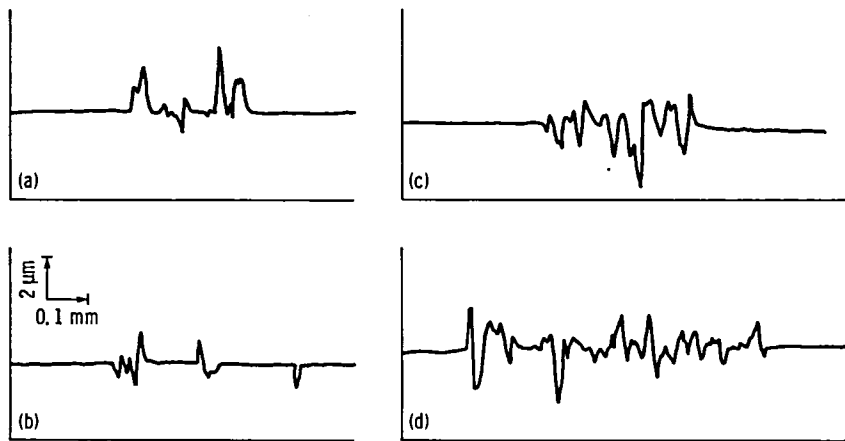
A typical topographical representation of a sliding track is illustrated in figure 18, which is based on the top photograph of figure 14. The topography of the sliding track has indications that wear fragments are separated from the edge of surface plateau, that the grooves develop, and that the plateau becomes smaller.

The distribution of the height for the surface contour from the figures is presented in figure 19. The distance from the initial height of the disk surface is reflected in the figure. The positive values for one-pass sliding represent, of course, the height of protuberances or material transferred to the sliding track, and the negative values denote the depth of the groove located just behind the protuberance. The positive value for 50 sliding passes represents the height of surface plateau, and the negative value indicates the depth of the groove located just behind the plateau with respect to the sliding direction. Therefore, for one-pass sliding, the negative value

5

(a) One pass; 10^{-6}-Pa vacuum.

(b) One pass; $5x15^{-4}$-Pa chlorine gas.

(c) 50 Passes; 10^{-6}-Pa vacuum.

(d) 50 Passes; $5x10^{-4}$-Pa chlorine gas.

Figure 7. - Surface profiles on disk surfaces after sliding experiments.
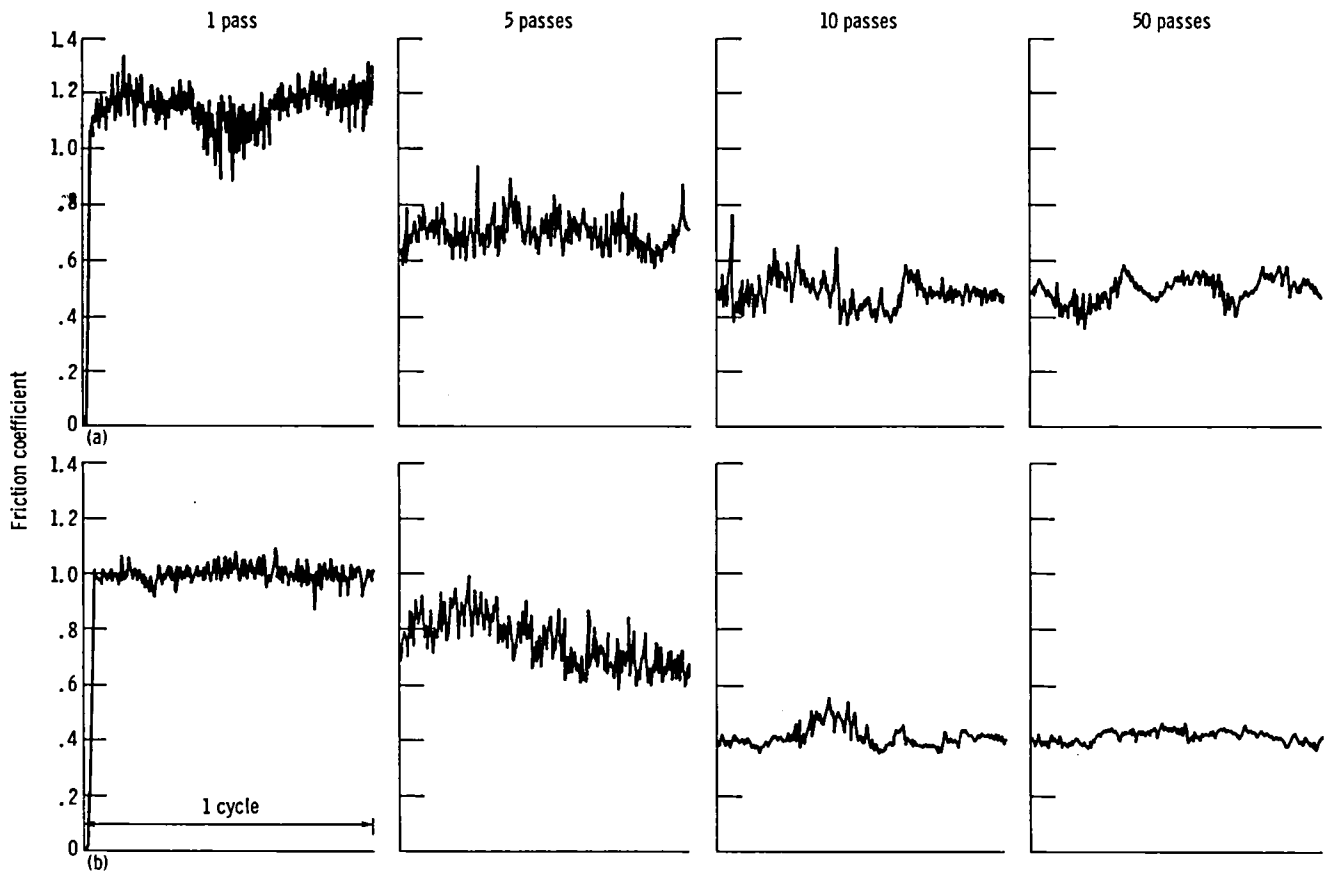
(a) Sliding environment, 10^{-6}-Pa vacuum.

(b) Sliding environment, $5x10^{-4}$-Pa chlorine gas.

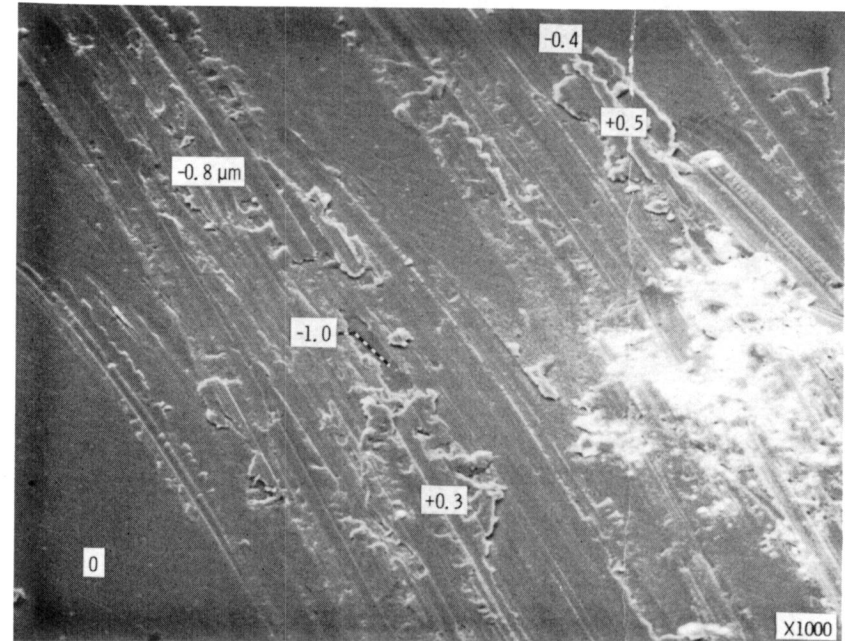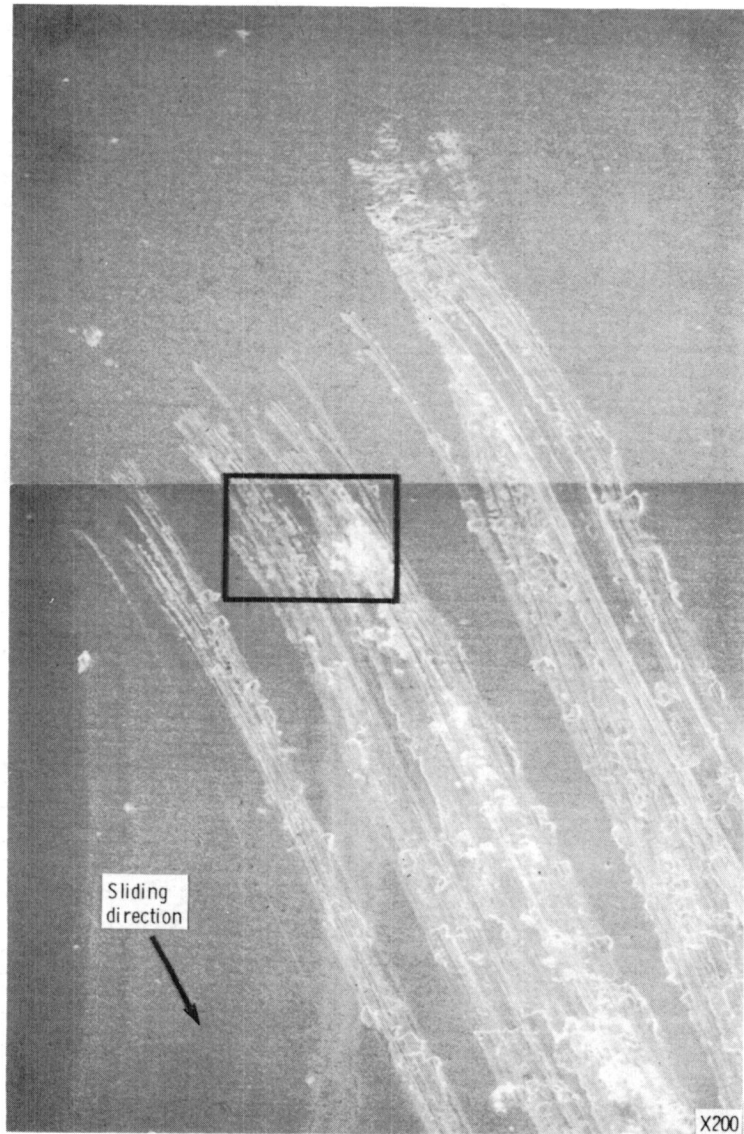Figure 8. - Variation of friction coefficient with number of sliding passes.

Figure 9. – Plastic deformation on disk surface (I). Initial stage of one-pass sliding in 10^{-6}-Pa vacuum. Figures denote distance (in μm) from initial height of disk surface.
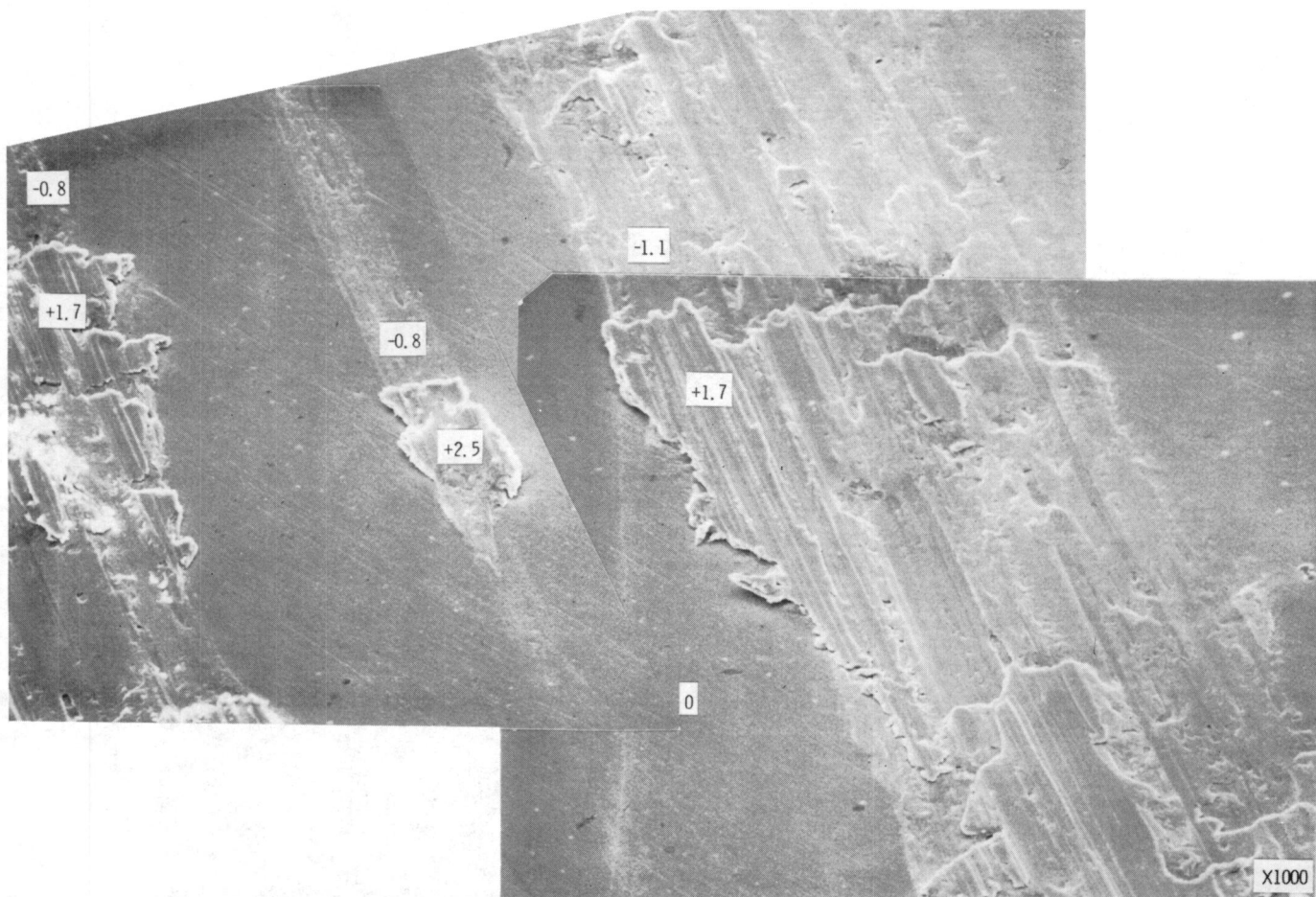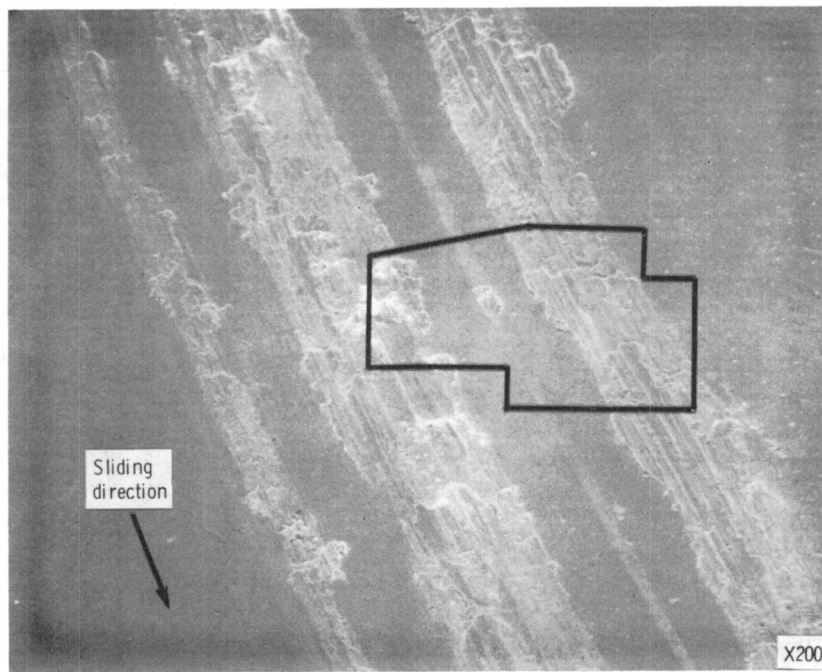
Figure 10. - Plastic deformation on disk surface (II). Later stage of one-pass sliding in 10^{-6}-Pa vacuum. Figures denote distance (in μm) from initial height of disk surface.
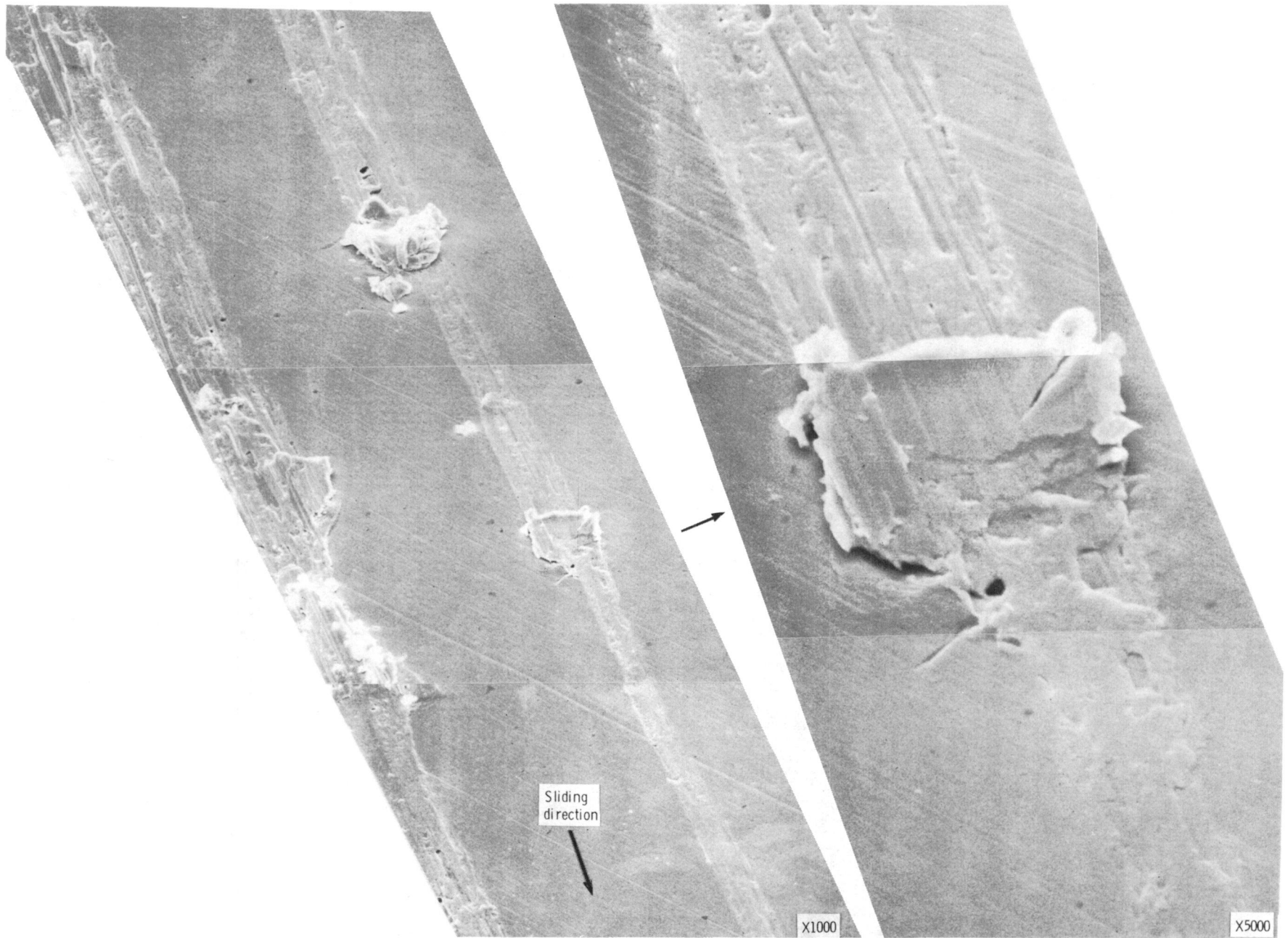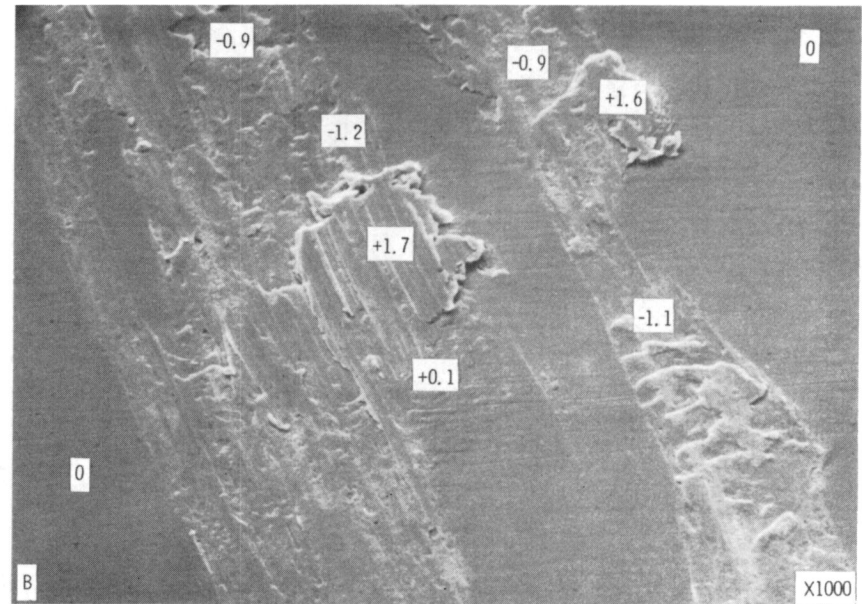
Sliding direction

X1000

X5000

Figure 11. - Plastic deformation on disk surface (III). Typical isolated mode of protuberances. One-pass sliding in 10^{-6}-Pa vacuum.

Sliding direction

X1000
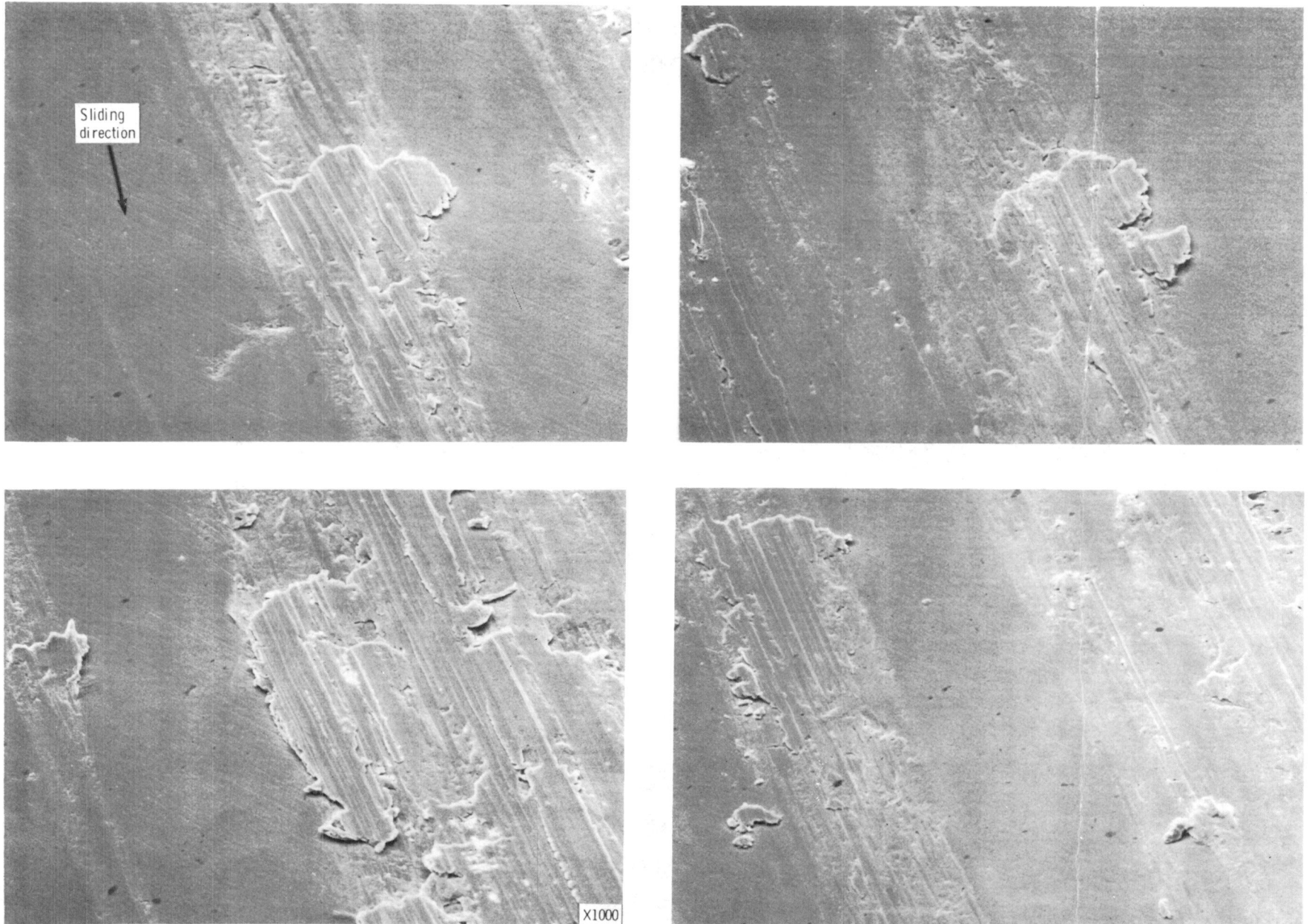
Figure 12. - Plastic deformation on disk surface (IV). Protuberances at various locations on sliding track. One-pass sliding in 10^{-6}-Pa vacuum.
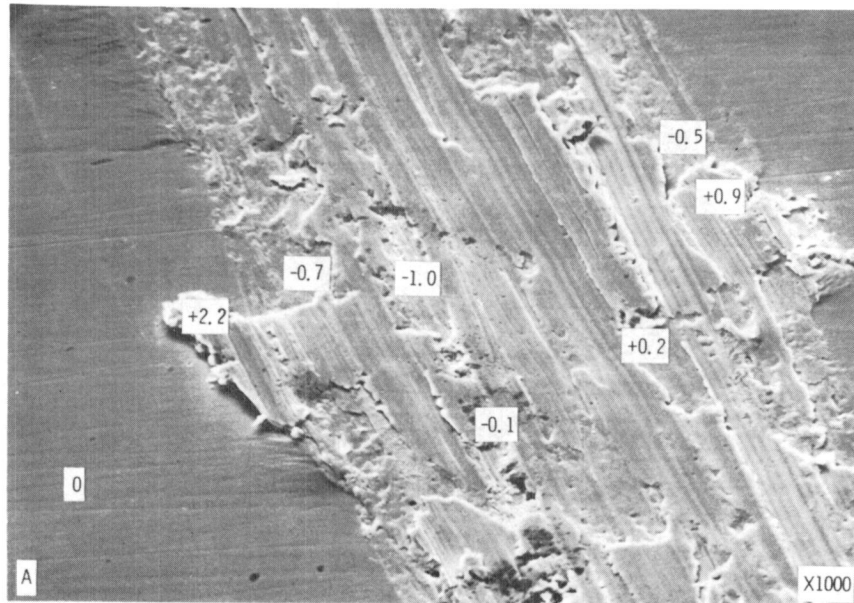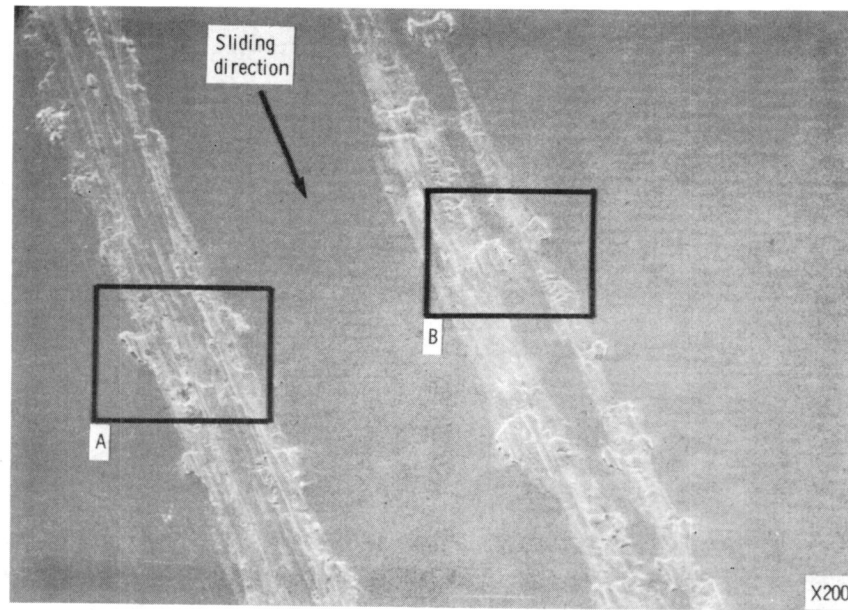
Figure 13. - Plastic deformation on disk surface (V). Later stage of one-pass sliding in 5×10^{-4}-Pa chlorine gas. Figures denote distance (in µm) from initial height of disk surface.
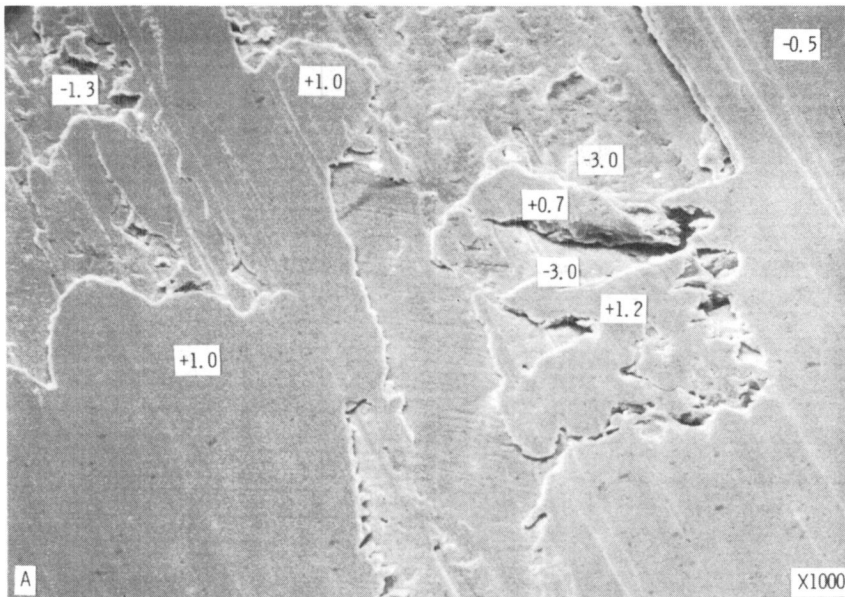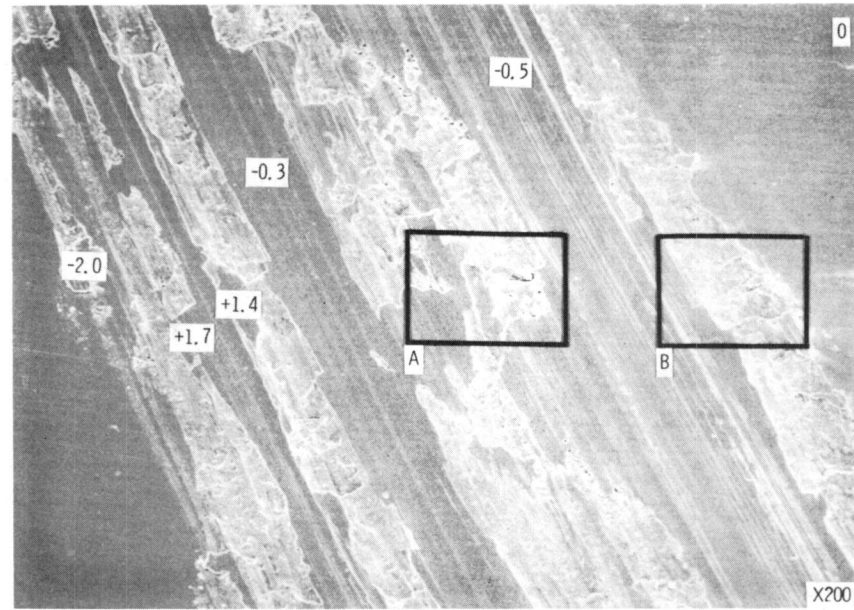
Figure 14. – Plastic deformation on disk surface (VI). 50-pass sliding in 10^{-6}-Pa vacuum. Figures denote distance (in µm) from initial height of disk surface.
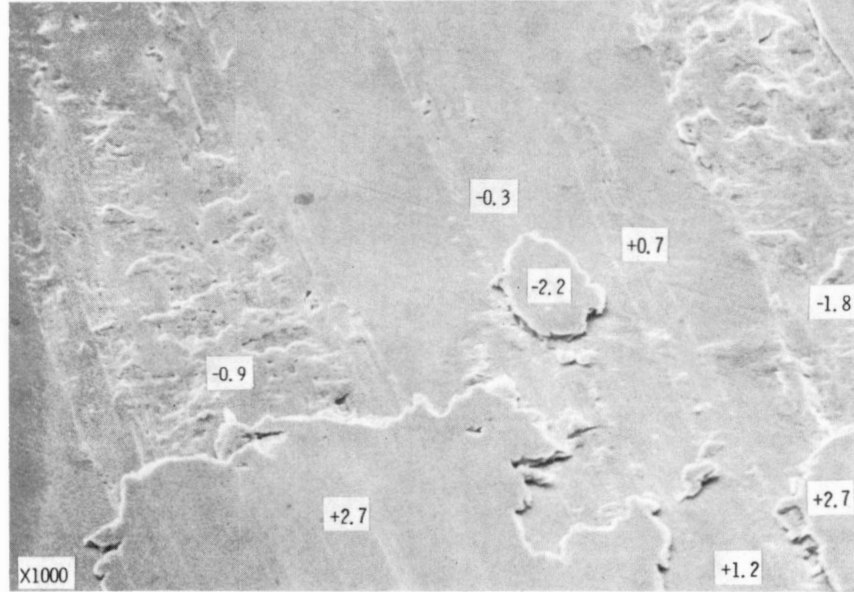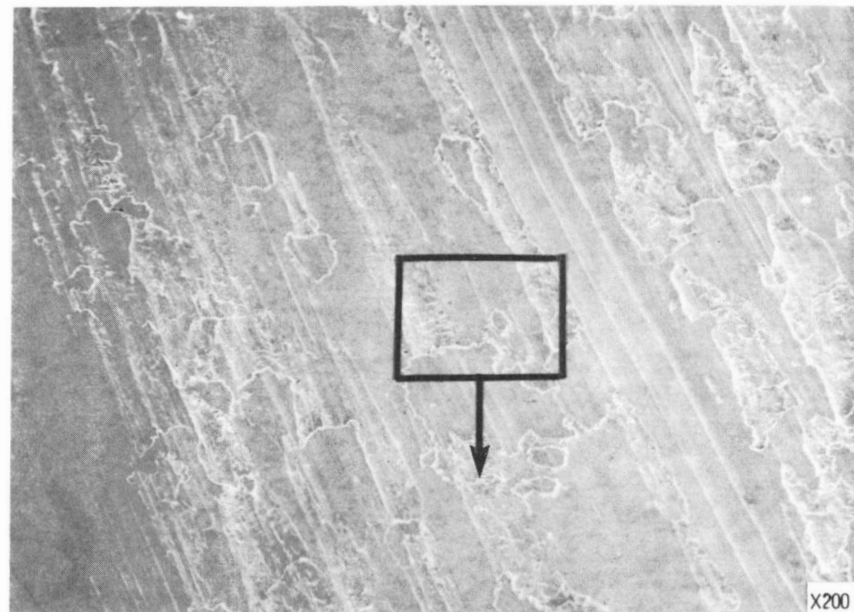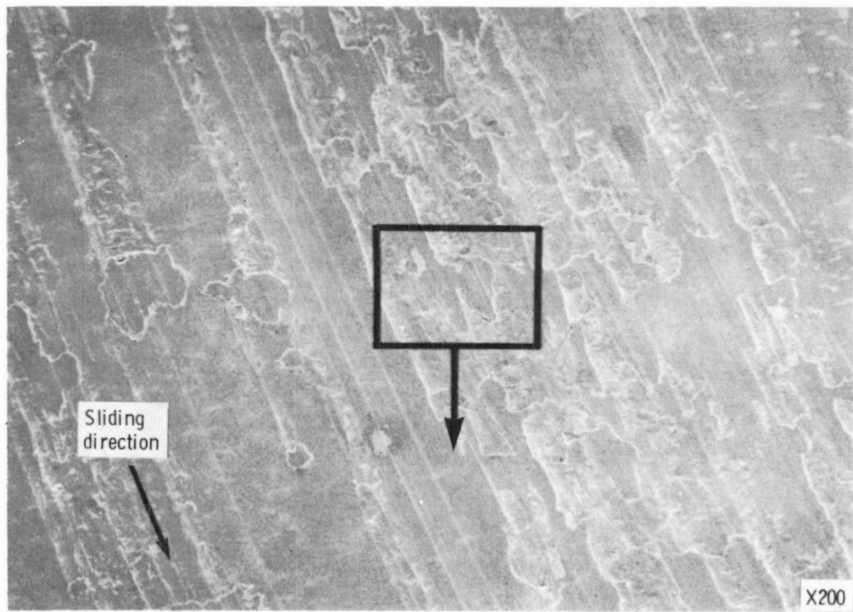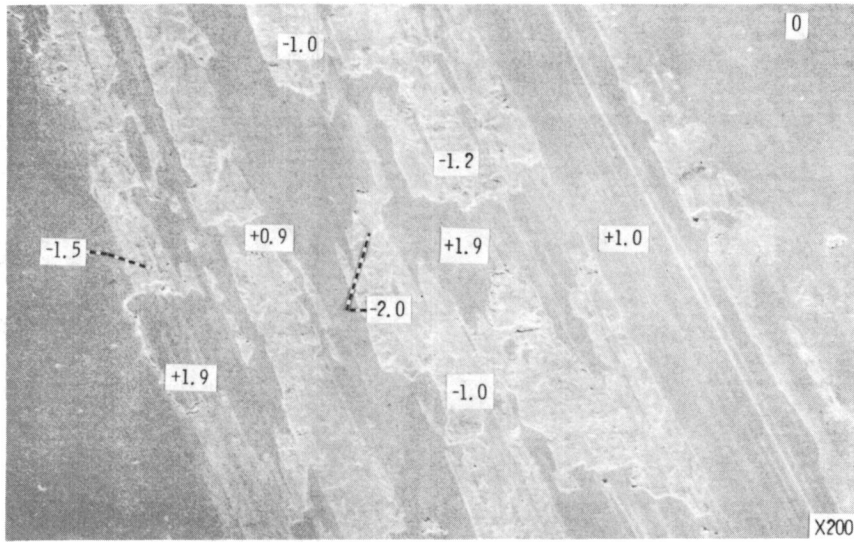
Figure 15. - Plastic deformation on disk surface (VII). 50-pass sliding in 5x10^{-4}-Pa chlorine gas. Figures denote distance (in μm) from initial height of disk surface.
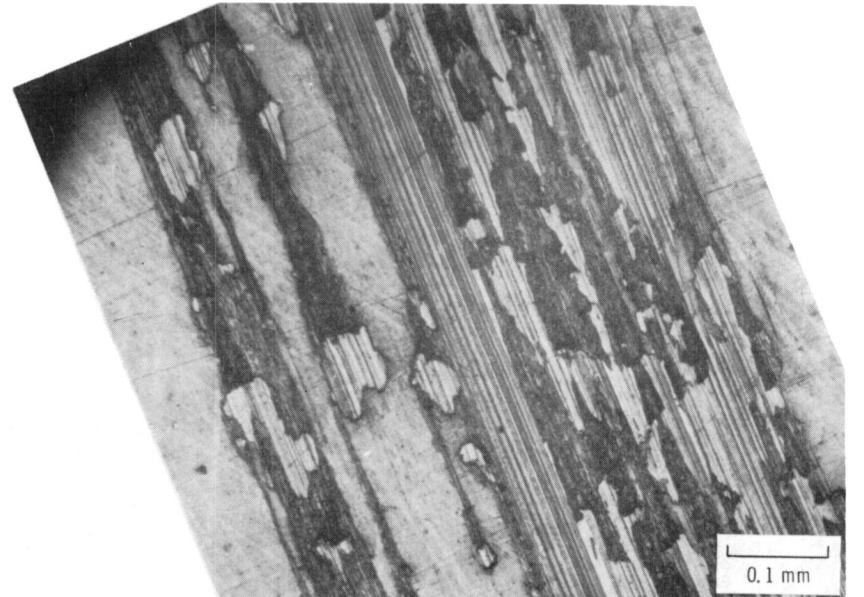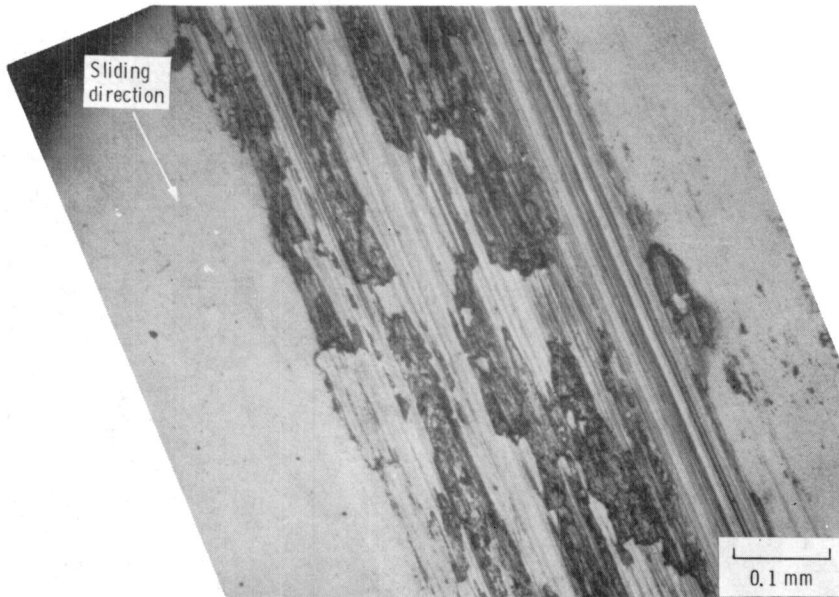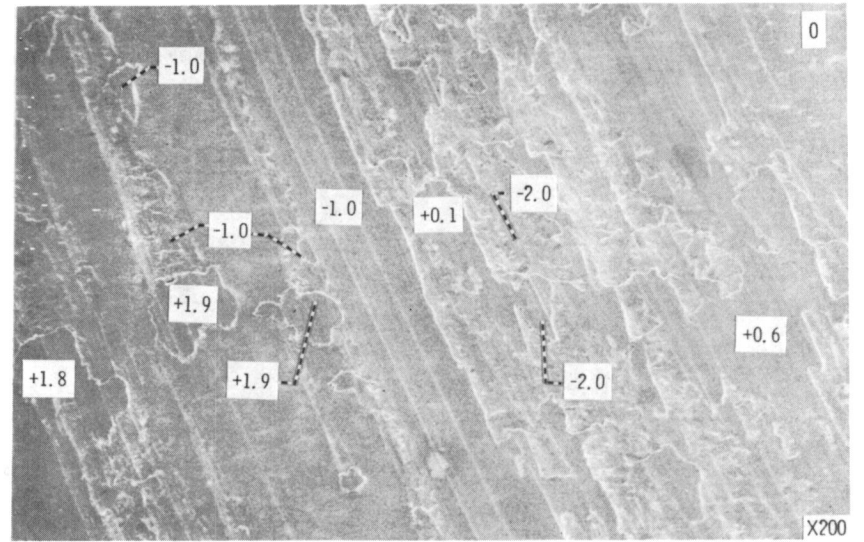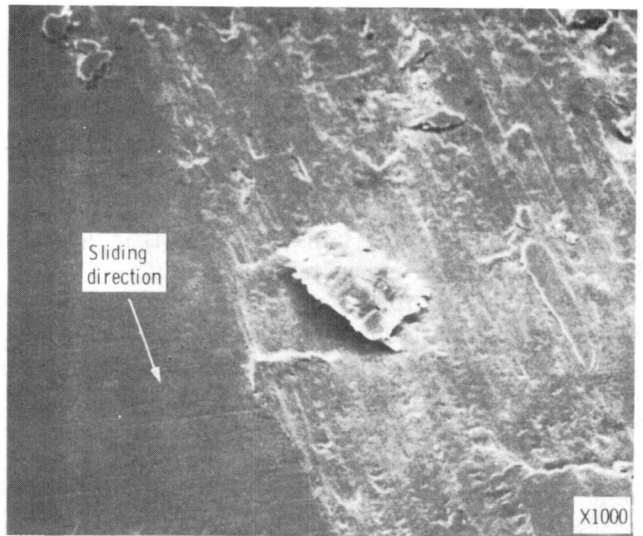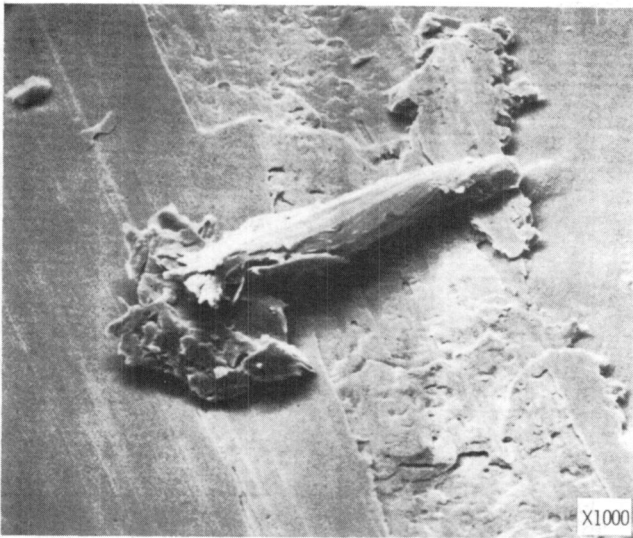
13

(SEM)

(a) 10^{-6}-Pa vacuum.

(b) 5x10^{-4}-Pa chlorine gas.

Figure 16. – Comparison of sliding tracks on disk surfaces after 50 passes. Figures denote distance (in μm) from initial height of disk surface.

(a) 50 Passes; 10^{-6}-Pa vacuum.

(b) 50 Passes; 5×10^{-4}-Pa chlorine gas.

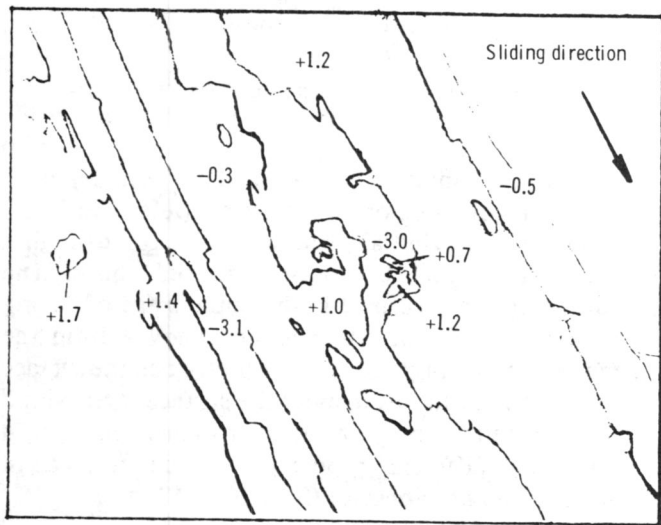Figure 17. - Examples of wear fragment observed in sliding track of disk.

Figure 18. - Topographical representation of sliding track. Figures denote distance (in µm) from initial height of disk surface.

Figure 19. - Height of protuberances and depth of grooves formed in sliding track.

indicates the depth of the primary shearing that forms the protuberance. The negative value for the 50-pass sliding implies the depth where the detachment that forms a wear fragment occurred.

Discussion

Characteristic modes of deformation and fracture were observed on the surface of 304 stainless-steel disks slid against aluminum oxide riders. Considering the groove, the shape of protuberances, and slip marks observed on the sliding track, we suggest the following mechanism for the formation of the step-shaped protuberances.

When surface interactions occur between disk and rider, the surface layer of the disk suffers shearing deformation by the tangential movement of the rider in the sliding process. The surfaces of practical material have a variety of geometric irregularity, unless created by some special techniques such as cleaving. The effective surface roughness is initially large, but smaller than the representative radius of curvature in the contact area. This roughness has a tendency to decrease because the transferred material fills in the valleys between asperities. There are, however, many asperities so inclined as to

15

engage each other across the interface in the sliding direction at early stages of the sliding process. This may be one reason for higher friction coefficient and its large fluctuation (fig. 8) in the early stages of sliding. Even when the contact changes into the metal-to-metal contact, owing to material transfer to the aluminum oxide rider, the interface brought about in this manner is apt to be inclined in a similar way, as is indicated by Cocks (ref. 3). In either case, adhesion is developed preferentially in these areas because the normal component of the sliding force is superposed in the areas.

Since the material involved in the adhesion process suffers plastic deformation, the material existing near the interface is generally work hardened. Furthermore, an interfacial adhesive bond, which occurs in the contact zone, is generally stronger than the cohesive bond in the cohesively weaker of the two materials. Based on these considerations, the shearing force necessary to separate the interface is usually larger than that of the material located below the interface. Therefore, the surface layer once adhered to the rider surface is sheared at a certain depth below the interface.

Real contact areas, incidentally, are generally scattered randomly in the apparent contact area. When an infinitesimal part of the surface layer deforms plastically within the real contact area, the deformation cannot extend to infinity in the tangential direction but is concentrated to a limited area. In other words, the deformation must be compensated for by the elevation of the localized surface layer. Therefore, the volume of material involved in the contact behavior expands both in the tangential and the vertical directions. The height of partially elevated surface increases gradually in this manner. These phenomena usually occur randomly in the apparent contact area, taking on different sizes and shapes. The rate of development in the vertical direction generally varies, depending on the area elevated. Since the mating aluminum oxide rider has a relatively smooth surface and since valleys of the asperities, even if they exist, will be filled with transferred material, partial elevations of the disk surface result in vertical movement of the aluminum oxide rider. Therefore, elevated areas will be separated by the vertical movement caused by the elevation at other areas.

The contact area where the specific contact stress exceeds a critical value will be pressed out and flattened on the "parent" surface by the rider during the sliding process. The former process is illustrated schematically in figure 20. The formation of characteristic modes of protuberances and slip marks observed on surfaces (figs. 9 to 13) can be well understood with the use of these mechanisms. More information is needed to fully understand the factors determining the height of the protuberances. The vertical displacement of the rider plays an important role in the formation of the

(1) - (2) Accumulation process
(3) - (4) Separation process
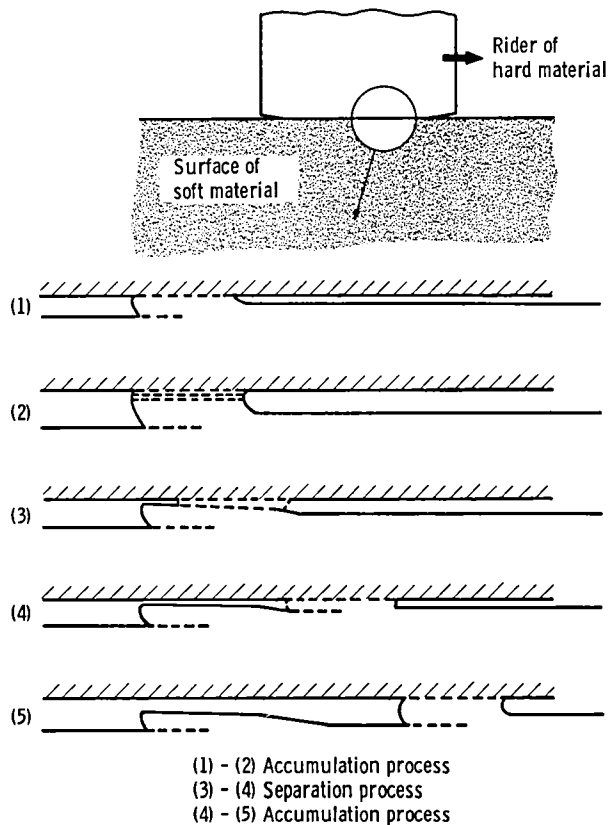(4) - (5) Accumulation process

Figure 20. - Formation process of protuberance.

protuberances. Similar phenomena have been reported for different combinations of materials (refs. 3 to 9).

The disk surface, initially smooth, will become rougher with repetitions of the process described above. The protuberances once formed in the initial stage of sliding contact have a chance either to be removed from the surface as a wear fragment or to be pressed on the surface and be flattened. In this manner the surface layer with a plateau-shaped configuration, probably having a mechanically different property, will be formed in subsequent sliding processes (figs. 14 to 18).

Conclusions

The deformation and wear process brought about at 304 stainless-steel disk surfaces slid against aluminum oxide riders was observed using a scanning electron microscope and an optical microscope. Experimental results are discussed in terms of adhesion.

The principal results obtained from the experiment are as follows:

1. The surface layer of the disk accumulates and is developed successively behind the rider. Step-shaped protuberances are set up in the initial steps of sliding contact even in a chlorine gas environment.

2. The primary shearing that forms the protuberance occurs in an extremely shallow region (1 μm below the contact surface).

3. The junction growth occurs in the vertical direction between the contact surfaces, which is an essential factor in producing the protuberances.

4. A matured surface layer develops at the contact surface and is predicted to be gradually torn off, taking a characteristic morphological contour in the sliding track.

5. The material separation producing wear fragments occurs at the depth of 2 to 3 micrometers.

Lewis Research Center,
National Aeronautics and Space Administration,
Cleveland, Ohio, February 18, 1982,

References

1. Buckley, D. H.: Surface Effects in Adhesion, Friction, Wear and Lubrication. Elsevier Publishing Co., 1981, pp. 245-313.
2. Bowden, F. P. and Tabor, D.: The Friction and Lubrication of Solids. Part II. Oxford University Press, 1964, pp. 87-107.
3. Cocks, M.: Interaction of Sliding Metal Surfaces. J. Appl. Phys., vol. 33, no. 7, July 1962, pp. 2152-2161.
4. Antler, M.: Wear, Friction and Electrical Noise Phenomena in Severe Sliding Systems. ASLE Trans., vol. 5, no. 2, Nov. 1962, pp. 297-307.
5. Cocks, M.: Role of Displaced metal in the Sliding of Flat Metal Surfaces. J. Appl. Phys., vol. 35, no. 6, June 1964, pp. 1807-1814.
6. Antler, M.: Process of Metal Transfer and Wear. Wear, vol. 7, 1964, pp. 181-203.
7. Cocks, M.: The Formation of Wedges of Displaced Metal Between Sliding Metal Surfaces. Wear, vol. 8, 1965, pp. 85-92.
8. Cocks, M.: Shearing of Junction between Metal Surfaces. Wear, vol. 9, 1966, pp. 320-328.
9. Sasada, T., Norose, S. and Mishina, H.: The Behavior of Adhered Fragments Interposed between Sliding Surfaces and the Formation Process of Wear Particles. J. Lubr. Technol., vol. 103, Apr. 1981, pp. 195-202.

1. Report No. NASA TP-2036	2. Government Accession No.	3. Recipient's Catalog No.
4. Title and Subtitle PLASTIC DEFORMATION AT SURFACE DURING UNLUBRICATED SLIDING		5. Report Date October 1982
		6. Performing Organization Code 506-33-12
7. Author(s) Takashi Yamamoto and Donald H. Buckley		8. Performing Organization Report No. E-1036
		10. Work Unit No.
9. Performing Organization Name and Address National Aeronautics and Space Administration Lewis Research Center Cleveland, Ohio 44135		
		11. Contract or Grant No.
		13. Type of Report and Period Covered Technical Paper
12. Sponsoring Agency Name and Address National Aeronautics and Space Administration Washington, D.C. 20546		
		14. Sponsoring Agency Code

16. Abstract

The plastic deformation and wear of 304 stainless-steel surface slid against an aluminum oxide rider were observed by using a scanning electron microscope and an optical microscope. Experiments were conducted in a vacuum of 10^{-6} Pa and in an environment of 5×10^{-4} Pa chlorine gas at 25° C. The load was 500 grams and the sliding velocity was 0.5 centimeter per second. The deformed surface layer which accumulates and develops successively is left behind the rider, and step-shaped protuberances are developed even after single pass sliding under both environmental conditions. A fully developed surface layer is gradually torn off leaving a characteristic pattern. These observations result from both adhesion and an adhesive wear mechanism.

17. Key Words (Suggested by Author(s)) Plastic deformation; Wear; Adhesion; Adhesive wear; Sliding contact; 304 stainless steel; Aluminum oxide	18. Distribution Statement Unclassified - unlimited STAR Category 37

19. Security Classif. (of this report) Unclassified	20. Security Classif. (of this page) Unclassified	21. No. of Pages 19	22. Price* A02

National Aeronautics and
Space Administration

Washington, D.C.
20546

THIRD-CLASS BULK RATE

U.S.MAIL

NASA